

Received June 7, 2020, accepted July 6, 2020, date of publication July 9, 2020, date of current version July 22, 2020.

Digital Object Identifier 10.1109/ACCESS.2020.3008209

Operation-Adaptive Damage Assessment of Steam Turbines Using a Nonlinear Creep-Fatigue Interaction Model

WOOSUNG CHOI¹, HEONJUN YOON², AND BYENG DONG YOUN^{3,4,5}, (Member, IEEE)

¹Research and Development Strategy Office, KEPSCO Research Institute, Daejeon 34056, South Korea

²George W. Woodruff School of Mechanical Engineering, Georgia Institute of Technology, Atlanta, GA 30332-0405, USA

³Department of Mechanical and Aerospace Engineering, Seoul National University, Seoul 08826, South Korea

⁴Institute of Advanced Machines and Design, Seoul National University, Seoul 08826, South Korea

⁵OnePredict Inc., Seoul 08826, South Korea

Corresponding author: Byeng Dong Youn (bdyoun@snu.ac.kr)

This work was supported in part by the 2017 Open Research and Development Program of Korea Electric Power Corporation (KEPCO) under Grant R17H02, and in part by the National Research Foundation of Korea (NRF) funded by the Korea Government (MSIT) under Grant 2020R1A2C3003644.

ABSTRACT For sustainable operation, power plants require accurate damage assessment of the steam turbines used for power generation. In the past few decades, steam turbine designs have considered only steady-state operation, without accounting for thermal cyclic loads. However, steam turbines designed for steady-state operation are often subjected to operation under cyclic and transient operation as well; this situation can cause both creep and fatigue damage. Creep and fatigue damage can interact with each other, thereby significantly impacting performance and leading to premature failure. Thus, this study proposes operation-adaptive damage assessment for steam turbines using a nonlinear creep-fatigue interaction model. The three-fold novel aspects of this study include methods to: 1) adaptively determine the hyper-parameters embedded in the nonlinear creep-fatigue interaction model depending on the operation mode (i.e., base-load and peak-load); 2) incorporate actual operation data acquired from field-deployed steam turbines; and 3) interpret the creep-fatigue damage interaction diagram with respect to the operation modes. It can be concluded from the results that the nonlinear creep and fatigue damage interaction is significantly affected by the operation mode as well as by the type of dominant damage mechanism.

INDEX TERMS Steam turbine, operation-adaptive damage assessment, cumulative damage rule, nonlinear creep-fatigue interaction model.

I. INTRODUCTION

Power generation companies have built supercritical steam turbine units with large capacity and high efficiency to reduce greenhouse gas (e.g., CO₂) emissions [1]. However, deterioration of steam turbine units can become accelerated as the operating time of the unit gets closer to reaching the end of its design life. Unplanned shutdown of a power plant due to accelerated degradation or unexpected failure can lead to considerable financial losses as well as potential widespread, even nationwide disaster [2]. Therefore, accurate damage assessment of critical components susceptible to failure is necessary for effective operation and maintenance of steam turbines [3]–[6].

The associate editor coordinating the review of this manuscript and approving it for publication was Zhenbao Liu¹.

According to failure mode and effect analysis (FMEA) of steam turbines, a turbine's high-intermediate pressure (HIP) rotor is a critical component due to its high risk. Fig. 1 shows the schematic of a HIP rotor. It is known that 'creep' and 'low-cycle fatigue (LCF)' are major failure mechanisms of HIP rotors [7]–[9]. When the operating temperature is beyond 30% of the absolute melting temperature of metallic materials, creep damage can accumulate significantly. Creep damage can produce large deformations, stress relaxation, and crack initiation and growth [10]. On the other hand, during operation, fatigue damage can be caused by repeated stress beyond (low-cycle) or below (high-cycle) the yield strength of the material, especially at stress concentration configurations (e.g., holes, fillets, and notches). Fatigue damage results in localized plastic deformations at stress concentration configurations [11]. As shown in Fig. 1, creep damage, which

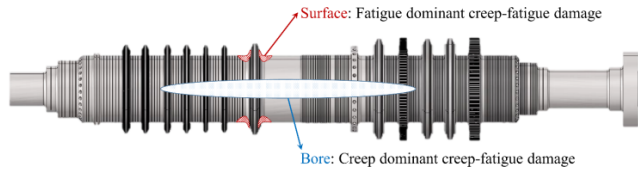


FIGURE 1. Schematic of a high-intermediate pressure (HIP) rotor and its damage mechanisms.

is dominant at the bore of the HIP rotor, is mainly caused by high temperature and centrifugal forces. Fatigue damage, which is dominant at the wheel root surface, is mainly caused by thermal cyclic loads due to frequent start-ups and shut-downs [12].

The operation modes of steam turbines can be categorized into the ‘base-load mode’ (steady-state operation) and the ‘peak-load mode’ (transient operation). In general, a base-load steam turbine in a coal-fired power plant runs continuously throughout a year. On the other hand, a peak-load steam turbine in a combined-cycle power plant runs only during the periods of peak demand for electricity; thereby, it experiences frequent start-ups and shut-downs [13]. This implies that creep damage is a primary concern for turbines under steady-state operation, while fatigue damage should be taken into consideration for turbines under transient operation. In the past few decades, when designing steam turbines, engineers have considered only steady-state operation, without accounting for thermal cyclic loads [14]. Recently, however, even steam turbines designed for steady-state operation are being asked to operate under cyclic and transient operation as well [15]; this situation can cause creep and fatigue damage in combination. Furthermore, increased operating temperatures are being proposed to improve the efficiency of combined-cycle power plants [1]; however, the durability of the main components against thermal fatigue must be ensured in these higher temperature settings [16], [17]. In other words, even though the dominant damage mechanisms might be different depending on the location (i.e., the bore and/or the wheel root surface), these mechanisms can interact with each other, thereby causing significant damage that can lead to premature failure.

Based on Miner’s rule, Lee *et al.* proposed a new life prediction method that considers fatigue and creep damage [18]. Miner’s linear damage accumulation method can be used for creep and fatigue damage assessment of steam turbines, however, it is only applicable when damages are independent of each other and do not overlap [19]. For the nonlinear creep-fatigue interaction model proposed by Rusin [20], all the hyper-parameters are assumed to be fixed under conservative assumptions; thereby, the operation modes cannot be considered. These limitations of existing methods drive research interest in developing a methodology for damage assessment of steam turbines that considers the ‘nonlinear creep-fatigue interaction’, while accounting for the operation mode.

Thus, this study aims to develop a methodology for operation-adaptive damage assessment of steam turbines

using a nonlinear creep-fatigue interaction model. The three-fold novel aspects of this study include: (1) adaptive determination of the hyper-parameters embedded in the nonlinear creep-fatigue interaction model depending on the operation mode; (2) incorporation of actual operation data acquired from field-deployed steam turbines into damage assessment of the HIP rotor; and (3) interpretation of the creep-fatigue damage interaction diagram with respect to the operation modes.

The remainder of this paper is organized as follows. Section II presents an operation-adaptive nonlinear creep-fatigue interaction model for damage assessment of steam turbines. Section III describes the actual operation and damage data acquired from field-deployed steam turbines. The performance of the proposed operation-adaptive nonlinear creep-fatigue interaction model is evaluated in Section IV. Finally, Section V outlines the conclusions of this study.

II. OPERATION-ADAPTIVE NONLINEAR CREEP-FATIGUE INTERACTION MODEL

This section proposes a nonlinear creep-fatigue interaction model for damage assessment of steam turbines. After briefly reviewing creep and fatigue damage models in Sections II.A and B, respectively, Section II.C describes the nonlinear creep-fatigue interaction model.

A. CREEP DAMAGE MODEL

1) STEADY-STATE STRESS FOR CREEP DAMAGE CALCULATION

When the HIP rotor rotates at a high speed, centrifugal forces are induced. Creep damage is mainly caused by the high temperature and centrifugal forces at the bore of the HIP rotor. It is well known that simplified methods can be used to calculate the stress with acceptable predictive capability, by replacing the complicated shape of the rotor with a hollow cylinder [21]–[24]. For a hollow cylinder, the radial and circumferential stresses, denoted by σ_r and σ_θ , are calculated by equations (1) and (2), respectively, as:

$$\sigma_r = \frac{(3 + \nu) \rho \omega^2}{8} \left(r_i^2 + r_o^2 - r^2 - \frac{r_i^2 r_o^2}{r^2} \right) \quad (1)$$

$$\sigma_\theta = \frac{(3 + \nu) \rho \omega^2}{8} \left\{ r_i^2 + r_o^2 - \left(\frac{1 + 3\nu}{3 + \nu} \right) r^2 + \frac{r_i^2 r_o^2}{r^2} \right\} \quad (2)$$

where r_i and r_o denote the inner (at the bore) and outer (at the surface) boundaries; ρ denotes the mass density; ω denotes the angular speed; and ν denotes the Poisson’s ratio. The radial stress is zero at both the bore and surface. This implies that creep damage of the HIP rotor is mainly attributed to the circumferential stress.

The circumferential stresses at the bore and surface can be obtained, respectively, as:

$$\sigma_{\text{bore}} = \sigma_c|_{r=r_i} = \frac{\rho \omega^2}{4} \left\{ (3 + \nu) r_o^2 + (1 - \nu) r_i^2 \right\} \quad (3)$$

$$\sigma_{\text{surface}} = \sigma_c|_{r=r_o} = \frac{\rho\omega^2}{4} \left\{ (3 + \nu)r_i^2 + (1 - \nu)r_o^2 \right\} \quad (4)$$

Since the circumferential stress at the bore is larger than that at the surface, creep damage at the bore is more serious. The circumferential stresses obtained using equations (3) and (4) are used to estimate creep damage at the bore and surface, respectively, using the Larson-Miller parameter.

2) CREEP DAMAGE CALCULATION

One of the most commonly used creep damage models is the Larson-Miller parameter, denoted by P , [21] as:

$$P = T(C + \log t_r) \quad (5)$$

where T denotes the temperature; t_r denotes the creep failure time. For 1Cr1Mo1/4V rotor steels, a plot of stress and Larson-Miller Parameter resulted in a single plot, within limits of scatter, regardless of the time-temperature combination employed to derive the parameter. C is a material specific constant, which is often approximated as 20 [22]. Since the creep strain is a temperature-related value, the Larson-Miller parameter considers the temperature T . Remember that the mean steam temperature (about 540 °C) during steady-state operation is used to calculate the creep damage. The Larson-Miller parameter can be used to estimate the creep failure time at a given temperature and stress level. The creep failure time can be estimated by rearranging equation (5) as:

$$t_r = 10^{\frac{P}{T}-20} \quad (6)$$

If the creep strain varies with the stress, the creep stress can be calculated by using the creep strain and tensile strength relations at room temperature. The creep life is then obtained from the creep stress. Steady-state stress is used in the case of creep damage.

After calculating the creep failure time t_r , the creep damage rate, denoted by D_{creep} can be obtained by using the operating time t as:

$$D_{\text{creep}} = \frac{t}{t_r} \quad (7)$$

B. FATIGUE DAMAGE MODEL

1) TRANSIENT PEAK STRAIN FOR FATIGUE DAMAGE CALCULATION

Fatigue damage, which is dominant at the wheel root surface, is mainly caused by thermal cyclic loads that arise due to frequent start-ups and shut-downs. Therefore, thermal strain under transient operation needs to be calculated to assess fatigue damage of the HIP rotor, while accounting for stress concentration factors at the critical regions [22].

During start-up or shut-down, the thermal stress or strain of the steam turbine can be calculated by finite element analysis. However, it is difficult to incorporate these complex turbine rotor components into the finite element code to simulate stress, strain, and temperature histories. To reduce the calculation costs, an approximation method was proposed to assess fatigue damage of the turbine rotor [9]. The thermal

strains corresponding to the transient peak-load operation mode, as well as the stress and strain concentration factors at the critical regions, need to be calculated. Based on the approximate relationship between the thermal strain, geometric information, and material properties, the thermal strains at the surface and bore can be calculated. The dimensionless nominal thermal stress, denoted by C_{max} , on the surface and bore of the HIP rotors can be expressed with the actual maximum thermal stress σ_{max} [22], [23] as:

$$C_{\text{max}} = -\frac{(1 - \nu)\sigma_{\text{max}}}{E\alpha_T\Delta T} \quad (8)$$

where E denotes the Young's modulus; α_T denotes a thermal expansion coefficient (12.5 W/m°C at 500 °C); ΔT denotes the maximum temperature difference; and σ_{max} denotes the actual maximum thermal stress. The total (elastic-plastic) strain can be obtained by multiplying the dimensionless nominal thermal stress by the plastic strain concentration factor, denoted by K_ϵ , as:

$$\Delta\epsilon_t = K_\epsilon C_{\text{max}} \quad (9)$$

The plastic strain concentration factor is a function of the thermal stress concentration factor; the detailed procedure used to calculate the plastic strain concentration factor can be found in [24]. The transient peak strain obtained in equation (9) is used to calculate fatigue damage by finding the Coffin-Manson relationship.

2) FATIGUE DAMAGE CALCULATION

The relationship between the LCF life, denoted by N_t , and the total strain, denoted by $\Delta\epsilon_t$, is proposed by Coffin [25], which is expressed as:

$$\Delta\epsilon_t = \epsilon_e + \epsilon_p = Q_1 N_t^{h_e} + Q_2 N_t^{h_p} \quad (10)$$

where ϵ_e and ϵ_p are the elastic and plastic strains, respectively. And Q and h are parameters determined by materials for the elastic and plastic strain. After calculating the LCF life N_t , the fatigue damage rate, denoted by D_{fatigue} can be obtained by using the number of cycles N as:

$$D_{\text{fatigue}} = \frac{N}{N_t} \quad (11)$$

Since the LCF life is determined by using the total strain $\Delta\epsilon_t$ under transient operation, it is necessary to consider the cold, warm, and hot start-up modes individually to calculate the LCF life. In other words, the dimensionless nominal thermal stress in equation (8) should be calculated according to each start-up mode; then, the corresponding actual strain and fatigue damage rate are determined. Finally, the total or cumulative fatigue damage rate can be obtained by summing the fatigue damage rates calculated for each start-up mode.

C. CREEP-FATIGUE INTERACTION MODEL

Due to its simplicity, Miner's linear damage accumulation method is a popular approach for creep and fatigue damage

assessment. Creep and fatigue damage can be evaluated by a linear summation rule as:

$$D = D_{\text{creep}} + D_{\text{fatigue}} \quad (12)$$

The linear cumulative damage rule is generally used to predict the lifetime of power plant components such as rotors, casings, and valves [26]–[29]; however, this approach is only applicable when the types of damage are independent of each other and do not overlap [19]. To overcome this limitation of linear damage models, this study implements a nonlinear continuum damage mechanics model to assess creep-fatigue damage of the HIP rotor [30]. The nonlinear creep-fatigue interaction model [20] for damage assessment can be expressed as:

$$D = aD_{\text{creep}} + bD_{\text{fatigue}} + \alpha (D_{\text{creep}} \cdot D_{\text{fatigue}})^\beta \quad (13)$$

where a , b , α and β are the hyper-parameters related to creep-fatigue interactions. In the published literature [20], a and b are assumed to be fixed to 1 to have equal weights for creep and fatigue damages in linear creep-fatigue interaction models. The hyper-parameter α and β that determine the nonlinear interaction effects are assumed to be fixed to certain values under conservative assumptions; thereby, actual operation conditions cannot be considered. In this study, however, it is worth pointing out that the hyper-parameters α and β in equation (13) are determined adaptively, according to the operation mode (i.e., the base-load and peak-load). Thus, our approach enables operation-adaptive damage assessment of steam turbines that considers nonlinear creep-fatigue interactions. This feature is one novelty of our approach.

III. DESCRIPTION OF ACTUAL OPERATION AND DAMAGE DATA

This section describes the actual operation and damage data. To obtain the operating time t in equation (7) and the number of cycles N in equation (11), this study incorporates actual operation data acquired from field-deployed, large-scale steam turbines. Section III.A describes the actual operation data, while Section III.B describes the creep and fatigue damage data.

A. ACTUAL OPERATION DATA

Actual operation data contain a variety of information that cannot be easily collected in a testbed in a laboratory. Fig. 2 describes the typical real-time database (RTDB) obtained from a supercritical steam turbine, including the main steam temperature, the 1st-stage temperature, the power output, and the turbine speed under a typical in-service loading condition of a power plant. Here, the increasing rate of the main steam temperature is incorporated into calculating the fatigue damage during the start-up stage (transient), while the mean steam temperature (about 540 °C) during steady-state operation is used to calculate the creep damage. The start-up stage can be classified into cold, warm, and hot start-up modes. Furthermore, it is necessary to consider each start-up mode to

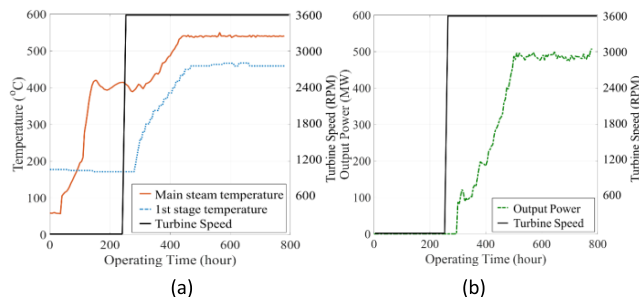


FIGURE 2. Typical real-time database (RTDB) obtained from a supercritical steam turbine: (a) main steam temperature, 1st-stage temperature, and (b) output power.

calculate the LCF life; the stress is calculated in accordance with the start-up mode and fatigue damage is determined correspondingly. Then, the total fatigue damage can be obtained by accumulating the fatigue damage rate for each start-up mode.

TABLE 1. Operation history of steam turbine.

Type	Coal-fired power plant				Combined power plant	
Mode	Base-load				Peak-load	
Steam turbine unit	B1	B2	B3	B4	P1	P2
Output power (MW)	500	500	500	500	182	200
Equivalent operating time (hour)	74,327	95,097	115,671	157,995	201,671	213,175
Number of cycles	39	58	122	134	556	582

Table 1 summarizes the operation histories of coal-fired and combined power plants. Base-load steam turbines in a coal power plant run continuously throughout a year, while peak-load steam turbines in a combined-cycle power plant run only during the periods of peak demand for electricity. This implies that steam turbine units operate with different fuel sources and power outputs, as shown in Table 1. To the best of the authors’ knowledge, this is the first time a model has been devised that incorporates real operation data into creep-fatigue damage interaction assessment of steam turbines.

B. CREEP AND FATIGUE DAMAGE DATA

In this study, a test dataset from NIMS (the National Institute on Materials Science, Japan) was used for 1Cr1Mo1/4V rotor steel [31], [32]. It is well known that a laboratory specimen of 1Cr1Mo1/4V rotor steel at 565 °C is suitable to evaluate creep-fatigue damage of HIP rotors [33]. In the case of 1Cr1Mo1/4V rotor steel, the coarsening of carbides and the annihilation and rearrangement of dislocation tend to occur under long-term, high temperature operation, thereby resulting in softening.

Figure 3 (a) shows the creep rupture test data of a 1Cr1Mo1/4V rotor steel specimen. These data contain

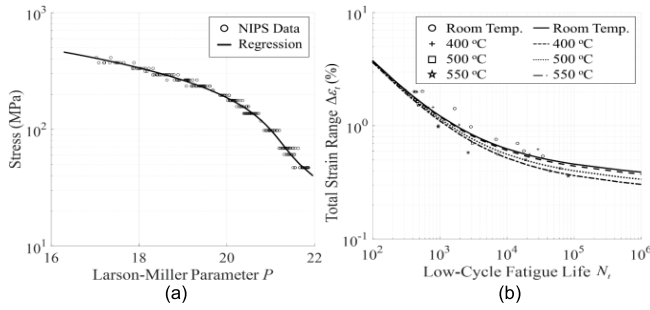


FIGURE 3. (a) Creep rupture test data (b) Low cycle fatigue test data of 1CrMo1/4V rotor steel.

information on the functional relation between the Larson-Miller parameter and stress; here, the stress and P relationship is normally described as a convex nonlinear curve. For a simple calculation, this functional relation can be expressed by using a multiple regression method as:

$$P(\sigma) \cong A_1 + A_2(\log \sigma) + A_3(\log \sigma)^2 + A_4(\log \sigma)^3 \quad (14)$$

where $A_1 = 11.483$, $A_2 = -24.204$, $A_3 = -21.394$, and $A_4 = -6.895$ for a 1CrMo1/4V rotor steel. Note that the Larson-Miller parameter is expressed as a function of the stress. Then, using equation (6), the Larson-Miller parameter can be used to calculate the creep failure time. Fig. 3 (b) shows the LCF fatigue test data of a 1CrMo1/4V rotor steel at different temperatures; this contains information on the functional relation between the LCF life and total strain range. Here, both are described in a logarithmic scale. In equation (10), $Q_1 = 0.62994$, $Q_2 = 22$, $h_e = -0.04572$, and $h_p = -0.59$ for fatigue damage calculation of a 1CrMo1/4V rotor steel. It can be observed from Fig. 4 that the LCF lives decrease as the temperature increases.

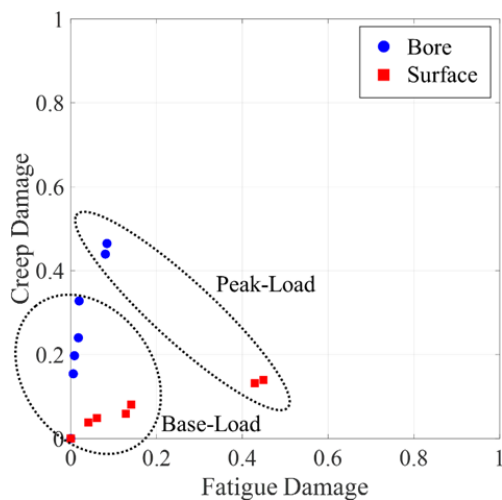


FIGURE 4. The trend of total damage with respect to the equivalent operating time.

Distribution types should be properly determined to statistically characterize the creep and fatigue damage data.

Based on the chi-square (χ^2), Komogorov-Smirnov (K-S), and Anderson goodness-of-fit (GoF) tests, lognormal and Weibull distributions were selected to statistically characterize the creep and fatigue damage data of 1CrMo1/4V rotor steel, respectively, as shown in Table 2. The statistical parameters were estimated using maximum likelihood estimation (MLE).

TABLE 2. The result of goodness-of-fit tests for the creep and fatigue data.

Damage mechanisms	Distribution type	p-value		
		Chi-Square	Kolmogorov-Smirnov	Anderson
Creep	Normal	0.1323	0.2643	0.1416
	Lognormal	0.4508	0.7663	0.9341
	Weibull	0.0699	0.2169	0.0809
Fatigue	Normal	0.4725	0.6871	0.6303
	Lognormal	0.2032	0.7219	0.9198
	Weibull	0.4648	0.8911	0.9432

IV. PERFORMANCE EVALUATION OF THE PROPOSED OPERATION-ADAPTIVE NONLINEAR CREEP-FATIGUE DAMAGE INTERACTION MODEL

This section is devoted to evaluating the performance of the proposed operation-adaptive nonlinear creep-fatigue damage interaction model. Section IV.A explains the estimation of the hyper parameters. After validating the proposed operation-adaptive creep-fatigue damage interaction model in Section IV.B, the effects of the operation mode on the nonlinear creep-fatigue interaction are discussed in Section IV.C.

A. ESTIMATION OF HYPER-PARAMETERS

In this study, the trust-region reflective least square method is implemented to estimate the unknown hyper-parameters α and β embedded in the nonlinear creep-fatigue interaction model in equation (13). The hyper-parameters are estimated in accordance with the operation mode (base-load and peak-load). The mean values of the estimated hyper-parameters are summarized in Table 3. Here, in order to investigate the nonlinear effects of the creep-fatigue damage interactions, a and b in equation (13) are set to be 1 under same conditions as [11]. The accuracy of the nonlinear creep-fatigue interaction model is evaluated by comparing the true data with the statistical distributions calculated by the damage model.

B. MODEL VALIDATION

The results obtained by the operation-adaptive creep-fatigue damage interaction model were compared with those derived from the two existing models (i.e., the linear model and the nonlinear interaction model with fixed hyper-parameters). In the comparison, material test data for turbine rotor steel during 157,995 hours and 213,175 hours of operation were used for the base-load (B4 Unit) and peak-load (P2 Unit) modes, respectively. The hyper-parameters embedded in the

TABLE 3. Mean values of the estimated interaction parameters.

Mode	Location (Dominant damage)	True damage	Linear model		Nonlinear model with the fixed hyper-parameters		Proposed nonlinear model	
			Est.	Error	Est.	Error	Est.	Error
Base-load	Surface (Fatigue)	0.6080	0.2217	63.6 %	0.3016	50.4 %	0.6218	11.8 %
	Bore (Creep)		0.3368	74.2 %	0.3769	74.2 %	0.6098	0.5 %
Peak-load	Surface (Fatigue)	0.8193	0.5886	28.2 %	0.7763	5.2 %	0.8209	0.2 %
	Bore (Creep)		0.5492	33.0 %	0.6977	14.8 %	0.8193	0.0 %

proposed nonlinear interaction model in equation (13) were estimated using nonlinear regression analysis.

TABLE 4. The results of damage assessment for each operation mode.

Mode	Location	Damage	Hyper-parameters		
			α	β	RMS
Base-load	Surface	Fatigue	1.213	0.279	0.974
	Bore	Creep	2.038	0.356	0.994
Peak-load	Surface	Fatigue	0.431	0.223	0.995
	Bore	Creep	0.312	0.044	0.994

Table 4 summarizes the results of damage assessment for the base-load and peak-load operation modes. The results of each damage rate according to the operation mode were compared with the true damage rates obtained from previous studies [7]. Note that creep damage is dominant at the bore of the HIP rotor, while fatigue damage is dominant at the surface. For the base-load mode, the creep and fatigue damage at the surface estimated using the existing linear model and nonlinear interaction model are 0.2217 and 0.3016, respectively; the errors are 63.6 % and 50.4 %, respectively. For the peak-load mode, the estimated results are in a good agreement with the observed results, compared to the base-load operation mode. On the other hand, it is worth pointing out that the mean values calculated by the proposed operation-adaptive creep-fatigue damage interaction model are in a very good agreement with the observed results regardless of the operation mode and the dominant damage mechanism. Thus, it can be concluded from the results that the proposed nonlinear creep-fatigue damage interaction model outperforms the existing models.

C. THE EFFECT OF THE OPERATION MODE ON THE NONLINEAR CREEP-INTERACTION

Figure 4 shows the trends of the mean values of total damage with respect to the equivalent operating time; the blue circle and red rectangular dots indicate the mean values of total damage at the bore and surface, respectively. The mean values of creep and fatigue damage are calculated using equations (7) and (11), respectively. Each dot corresponds

to the equivalent operating time in Table 1, in chronological order. At the beginning of operation, there is almost no damage; however, damage gradually increases with the equivalent operating time. As can be seen in Fig. 4, even though creep and fatigue damage occur simultaneously and interact each other, creep damage is relatively larger than fatigue damage at the bore over the entire equivalent operating time. Fatigue damage is relatively larger than creep damage at the surface over the entire equivalent operating time. As the damage rate tends to increase over time, in addition, the fatigue damage increase rate on the surface of turbine decreases as the operating time elapses. On the other hand, the creep damage increase rate at the bore which is the main damage mechanism is seen to increase over the equivalent operating time. This underscores the necessity of operation-adaptive damage assessment of steam turbines.

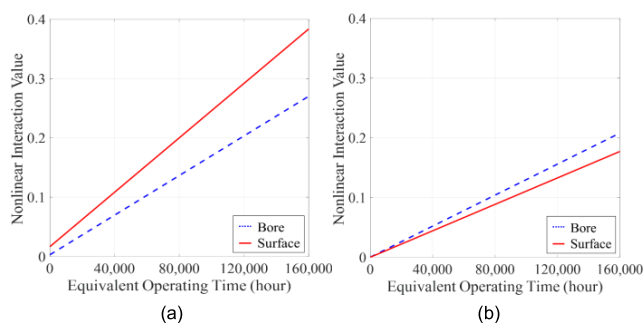


FIGURE 5. Nonlinear interaction value with the equivalent operating time: (a) base-load and (b) peak-load.

Figure 5 shows the nonlinear interaction value of creep and fatigue damage, which is calculated by the third term on the right-hand side in equation (13), with the equivalent operating time. The red solid line indicates the nonlinear interaction value at the surface, where fatigue damage is dominant; the blue dotted line represents the nonlinear interaction value at the bore, where creep damage is significant. Please note that the hyper-parameters in equation (13) are calculated adaptively according to the operation mode. Overall, the nonlinear interaction value under base-load operation (Fig. 5 (a)) is larger than that under peak-load operation (Fig. 5 (b)). It is worth pointing out that the nonlinear interaction value at the surface is larger than that at the bore under base-load operation, while it is smaller under peak-load operation. Thus, it can be concluded that the operation mode significantly affects the nonlinear creep and fatigue damage interaction. Fig. 5 ascertains the importance of considering the operation mode for accurate damage assessment of steam turbines.

Figure 6 shows the creep and fatigue damage interaction diagram under the base-load and peak-load modes. The linear model (black solid line) is only applicable when the damages are independent of each other. Furthermore, the nonlinear creep-fatigue damage interaction model with fixed hyper-parameters (gray dashed line) cannot account for the effect of the operation mode on the creep and fatigue damage interaction diagram. However, it is worth pointing out that the proposed nonlinear creep-fatigue damage interaction model

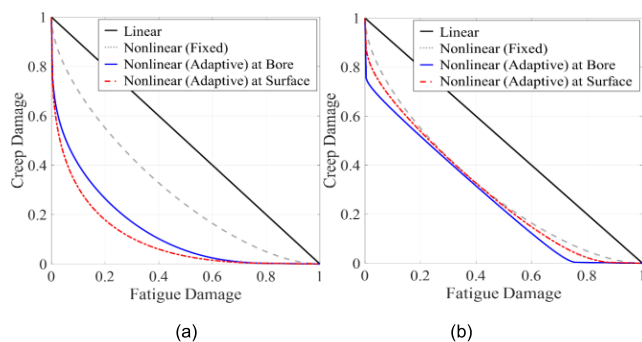


FIGURE 6. Creep and fatigue damage interaction diagram under: (a) base-load operation and (b) peak-load operation.

with the adaptive hyper-parameters clearly shows that the creep and fatigue damage interaction diagram is affected significantly by the operation mode as well as the type of dominant damage mechanism. In general, creep damage, which is dominant at the bore, is a primary concern under the base-load operation mode; creep damage is mainly caused by high temperature and centrifugal forces. Fatigue damage, which is dominant at the surface, should be taken into consideration under the peak-load operation mode; fatigue damage is mainly caused by thermal cyclic loads that are due to frequent start-ups and shut-downs. If a steam turbine designed for the base-load mode operates under the peak-load mode, the reduction of its lifetime is accelerated due to the nonlinear interaction at the bore, where fatigue damage is a concern.

Please note again that the hyper-parameters embedded in the proposed nonlinear creep-fatigue damage interaction model were determined adaptively in accordance with the operation mode (base-load or peak-load). In Fig. 6, the hyper-parameters for the base-load and peak-load modes were estimated using the operating history of steam turbine units of coal fired power plants (B1 to B4) and combined power plants (P1 and P2), respectively. The equivalent operating times of units B1 to B4 are shorter than those of units P1 and P2. This implies that the creep and fatigue damage interaction diagram under base-load operation is valid below a damage level of 0.4~0.6, while the diagram under peak-load operation is valid above that level.

V. CONCLUSION

Base-load steam turbines in a coal-fired power plant run continuously throughout a year, while peak-load steam turbines in a combined-cycle power plant run only during periods of peak demand for electricity. However, steam turbines designed for a base-load (steady-state) operation mode are often subjected to operation under a peak-load (cyclic and transient) operation mode as well. In other words, even though dominant damage mechanisms might be different depending on the location (i.e., the bore and the wheel root surface), these damage types can interact with each other, thereby causing significant damage that leads to premature failure. Thus, this study proposed a methodology

for operation-adaptive damage assessment of steam turbines using a nonlinear creep-fatigue interaction model. The three-fold novel aspects of this study include: 1) adaptive determination of the hyper-parameters embedded in the nonlinear creep-fatigue interaction model depending on the operation mode; 2) incorporation of actual operation data acquired from field-deployed steam turbines into damage assessment of the HIP rotor; and 3) interpretation of the creep-fatigue damage interaction diagram with respect to the operation mode.

Our research shows that the rate of increase of fatigue damage is slightly higher under peak-load operation (transient), while the rate of increase of creep damage is slightly higher under base-load operation. Furthermore, the nonlinear interaction value at the surface is larger than that at the bore under base-load operation, while the nonlinear interaction value is smaller under peak-load operation. From the results obtained by the proposed operation-adaptive, creep-fatigue damage interaction model, we identified three key findings: 1) for accurate damage assessment of steam turbines in which creep and fatigue damage occur simultaneously, their nonlinear interaction effects have to be taken into consideration; 2) the creep and fatigue damage interaction diagram is significantly affected by the operation mode as well as by the type of dominant damage mechanism; and 3) if a steam turbine designed for the base-load mode operates under the peak-load mode, its lifetime is reduced at an accelerated rate due to the nonlinear interaction at the bore, where fatigue damage occurs. Thus, it can be concluded that the proposed operation-adaptive, creep-fatigue damage interaction model can contribute to accurate damage assessment of steam turbines. Since accurate life prediction of aging steam turbines is becoming more important as the globally friendly energy policy requires operating a steam turbine designed as a base load at peak load, the results of this study can be useful for actual plant operation and maintenance.

REFERENCES

- [1] G. Nowak and A. Rusin, "Shape and operation optimisation of a supercritical steam turbine rotor," *Energy Convers. Manage.*, vol. 74, pp. 417–425, Oct. 2013.
- [2] I. Shin, J. Lee, J. Y. Lee, K. Jung, D. Kwon, B. D. Youn, H. S. Jang, and J.-H. Choi, "A framework for prognostics and health management applications toward smart manufacturing systems," *Int. J. Precis. Manuf.-Green Technol.*, vol. 5, no. 4, pp. 535–554, Aug. 2018.
- [3] H. Oh, J. H. Jung, B. C. Jeon, and B. D. Youn, "Scalable and unsupervised feature engineering using vibration-imaging and deep learning for rotor system diagnosis," *IEEE Trans. Ind. Electron.*, vol. 65, no. 4, pp. 3539–3549, Apr. 2018.
- [4] J. T. Yoon, B. D. Youn, M. Yoo, Y. Kim, and S. Kim, "Life-cycle maintenance cost analysis framework considering time-dependent false and missed alarms for fault diagnosis," *Rel. Eng. Syst. Saf.*, vol. 184, pp. 181–192, Apr. 2019.
- [5] W. Choi, H. Huh, B. A. Tama, G. Park, and S. Lee, "A neural network model for material degradation detection and diagnosis using microscopic images," *IEEE Access*, vol. 7, pp. 92151–92160, 2019.
- [6] R. Kannan, C. P. Tso, R. Osman, and H. K. Ho, "LCA-LCCA of oil fired steam turbine power plant in Singapore," *Energy Convers. Manage.*, vol. 45, no. 18, pp. 3093–3107, Nov. 2004.
- [7] W. Choi, B. D. Youn, H. Oh, and N. H. Kim, "A Bayesian approach for a damage growth model using sporadically measured and heterogeneous on-site data from a steam turbine," *Rel. Eng. Syst. Saf.*, vol. 184, pp. 137–150, Apr. 2019.

- [8] Y.-J. Sun, Y.-L. Wang, M. Li, and J. Wei, "Performance assessment for life extending control of steam turbine based on polynomial method," *Appl. Thermal Eng.*, vol. 108, pp. 1383–1389, Sep. 2016.
- [9] W.-S. Choi, E. Fleury, B.-S. Kim, and J.-S. Hyun, "Life assessment of steam turbine components based on viscoplastic analysis," *J. Solid Mech. Mater. Eng.*, vol. 2, no. 4, pp. 478–486, 2008.
- [10] H. Mao and S. Mahadevan, "Reliability analysis of creep-fatigue failure," *Int. J. Fatigue*, vol. 22, no. 9, pp. 789–797, 2000.
- [11] H. Yoon and B. D. Youn, "System reliability analysis of piezoelectric vibration energy harvesting considering multiple safety events under physical uncertainty," *Smart Mater. Struct.*, vol. 28, no. 2, Feb. 2019, Art. no. 025010.
- [12] M. Banaszekiewicz, "The low-cycle fatigue life assessment method for online monitoring of steam turbine rotors," *Int. J. Fatigue*, vol. 113, pp. 311–323, Aug. 2018.
- [13] R. Kehlhofer, F. Hanneemann, B. Rukes, and F. Stirnimann, *Combined-Cycle Gas & Steam Turbine Power Plants*. Oklahoma, OK, USA: Pennwell Books, 2009.
- [14] W. Z. Wang, P. Buhl, A. Klenk, and Y. Z. Liu, "The effect of in-service steam temperature transients on the damage behavior of a steam turbine rotor," *Int. J. Fatigue*, vol. 87, pp. 471–483, Jun. 2016.
- [15] J. Baran, "Redesign of steam turbine rotor blades and rotor packages—Environmental analysis within systematic eco-design approach," *Energy Convers. Manage.*, vol. 116, pp. 18–31, May 2016.
- [16] H. Song, J.-M. Lee, Y. Kim, S. Yang, S. Park, J.-M. Koo, and C.-S. Seok, "Life prediction method for thermal barrier coating of high-efficiency eco-friendly combined cycle power plant," *Int. J. Precis. Eng. Manuf.-Green Technol.*, vol. 6, no. 2, pp. 329–337, Apr. 2019.
- [17] Y. Kim, J.-M. Lee, H. Song, K. Han, J.-M. Koo, Y.-Z. Lee, and C.-S. Seok, "TBC delamination life prediction by stress-based delamination map," *Int. J. Precis. Eng. Manuf.-Green Technol.*, vol. 4, no. 1, pp. 67–72, Jan. 2017.
- [18] J.-M. Lee, S. Wee, J. Yun, H. Song, Y. Kim, J.-M. Koo, and C.-S. Seok, "Life prediction of IN738LC considering creep damage under low cycle fatigue," *Int. J. Precis. Eng. Manuf.-Green Technol.*, vol. 5, no. 2, pp. 311–316, Apr. 2018.
- [19] Y. Xiao, "A multi-mechanism damage coupling model," *Int. J. Fatigue*, vol. 26, no. 11, pp. 1241–1250, Nov. 2004.
- [20] A. M. Rusin, "Technical risk involved in long-term operation of steam turbines," *Rel. Eng. Syst. Saf.*, vol. 92, no. 9, pp. 1242–1249, Sep. 2007.
- [21] H. Kraus, *Creep Analysis*. New York, NY, USA: Wiley, 1980.
- [22] R. Viswanathan, "Life-assessment technology for fossil power plants," *Sadhana*, vol. 20, no. 1, pp. 301–329, Feb. 1995.
- [23] D. Gonyea, "Thermal stress concentration factors in large shafts," in *Thermal Fatigue of Materials and Components*. West Conshohocken, PA, USA: ASTM International, 1976.
- [24] W. Choi, K. Fujiyama, B. Kim, and G. Song, "Development of thermal stress concentration factors for life assessment of turbine casings," *Int. J. Pressure Vessels Piping*, vol. 98, pp. 1–7, Oct. 2012.
- [25] L. F. Coffin, "Fatigue at high temperature—prediction and interpretation," *Proc. Inst. Mech. Engineers*, vol. 188, no. 1, pp. 109–127, Jun. 1974.
- [26] L. Cui and P. Wang, "Two lifetime estimation models for steam turbine components under thermomechanical creep-fatigue loading," *Int. J. Fatigue*, vol. 59, pp. 129–136, Feb. 2014.
- [27] D. Hu, R. Wang, and G. Hou, "Life assessment of turbine components through experimental and numerical investigations," *J. Pressure Vessel Technol.*, vol. 135, no. 2, Apr. 2013, Art. no. 024502.
- [28] A. Rusin, "Assessment of operational risk of steam turbine valves," *Int. J. Pressure Vessels Piping*, vol. 81, no. 4, pp. 373–379, Apr. 2004.
- [29] K. Yagi, O. Kanemaru, K. Kubo, and C. Tanaka, "Life prediction of 316 stainless steel under creep-fatigue loading," *Fatigue Fract. Eng. Mater. Struct.*, vol. 9, no. 6, pp. 395–408, 1987.
- [30] J. JianPing, M. Guang, S. Yi, and X. SongBo, "An effective continuum damage mechanics model for creep-fatigue life assessment of a steam turbine rotor," *Int. J. Pressure Vessels Piping*, vol. 80, no. 6, pp. 389–396, 2003.
- [31] K. Sawada et al., *Data Sheets on the Elevated-Temperature Properties of 1Cr-1Mo-0.25V Steel Forgings for Turbine Rotors and Shafts (ASTM A470-8)*. Tsukuba, Ibaraki: National Institute for Materials Science, 1990.

- [32] Y. Furuya, H. Nishikawa, H. Hirukawa, N. Nagashima, and E. Takeuchi, *Data Sheets on Elevated-Temperature, Time-Dependent Low-Cycle Fatigue Properties of ASTM A470-8 (1Cr-1Mo-0.25V) Steel Forging for Turbine Rotors and Shafts*. Tsukuba, Ibaraki: National Institute for Materials Science, 1987.
- [33] S. Holdsworth, "Creep-fatigue failure diagnosis," *Materials*, vol. 8, no. 11, pp. 7757–7769, Nov. 2015.



WOOSUNG CHOI received the B.S. degree from Inha University, Incheon, South Korea, in 2003, the M.S. degree from KAIST, Daejeon, South Korea, in 2005, and the Ph.D. degree from Seoul National University, Seoul, South Korea, in 2018. He is currently a Principal Researcher with the KEPSCO Research Institute, Daejeon. He is also in charge of life and risk assessment for power plant and development of national standard for power generation industry (Korea Electric Power Industry Code). His research interests include prognostics and health management, multifidelity analysis with finite element analysis, and deep learning analysis.



HEONJUN YOON received the Ph.D. degree from Seoul National University, Seoul, South Korea, in 2018. He is currently a Postdoctoral Fellow with the Georgia Institute of Technology, Atlanta, GA, USA. He was a recipient of the two Best Thesis Awards from the KSME, in 2013 and 2018, several Best Paper Awards from the BAMN, in 2013, the KSNVE, in 2014, the ENGE, in 2016, the Featured Article from Smart Materials and Structures, in 2014, the First Place Winner from the Student Paper Competition, the KSME, in 2016, the Bronze Prize from KSME-SEMES Open Innovation Challenge, in 2016, the Outstanding Ph.D. Dissertation Award from the Department of Mechanical and Aerospace Engineering, Seoul National University, in 2018, the Young Scientist Award from the ASSMO, in 2018, and the PHM Society Data Challenge Competition Winner, in 2019.



BYENG DONG YOON (Member, IEEE) received the B.S. degree from Inha University, Incheon, South Korea, in 1996, the M.S. degree from KAIST, Daejeon, South Korea, in 1998, and the Ph.D. degree from The University of Iowa, Iowa City, IA, USA, in 2001. He is currently a Professor with the Department of Mechanical and Aerospace Engineering, Seoul National University, Seoul, South Korea. He was an Assistant Professor with the Department of Mechanical Engineering, University of Maryland, College Park. His research goal is to develop rational reliability and design methods based on mathematics, physics, and statistics for use in complex engineered systems, mainly focused on energy systems. His current research interests include reliability-based design, prognostics and health management (PHM), energy harvester design, and virtual product testing. He has garnered substantive peer-recognition resulting in notable awards, including the ASME IDETC Best Paper Awards, from 2001 to 2008, the ISSMO/Springer Prize for a Young Scientist, in 2005, the IEEE PHM Competition Winner, in 2014, the PHM Society Data Challenge Competition Winner, in 2014, 2015, 2017, and 2019, respectively, and so on.

...